

## Combustion characteristics and kinetic analysis of co-combustion between bag dust and pulverized coal

Tao Xu<sup>1</sup>, Xiao-jun Ning<sup>1</sup>, Guang-wei Wang<sup>1</sup>, Wang Liang<sup>1</sup>, Jian-liang Zhang<sup>1,2</sup>, Yan-jiang Li<sup>1</sup>, Hai-yang Wang<sup>1</sup>, and Chun-he Jiang<sup>1</sup>

1) School of Metallurgical and Ecological Engineering, University of Science and Technology Beijing, Beijing 100083, China

2) School of Chemical Engineering, The University of Queensland, St Lucia, QLD 4072, Australia

(Received: 15 May 2018; revised: 1 July 2018; accepted: 9 July 2018)

**Abstract:** The combustion characteristics of blast furnace bag dust (BD) and three kinds of coal—Shenhua (SH) bituminous coal, Pingluo (PL) anthracite, and Yangquan (YQ) anthracite—were obtained via non-isothermal thermogravimetry. The combustion characteristics with different mixing ratios were also investigated. The physical and chemical properties of the four samples were investigated in depth using particle size analysis, Scanning electron microscopy, X-ray diffraction, X-ray fluorescence analysis, and Raman spectroscopy. The results show that the conversion rate of the three kinds of pulverized coals is far greater than that of the BD. The comprehensive combustion characteristics of the three types of pulverized coals rank in the order SH > PL > YQ. With the addition of BD, the characteristic parameters of the combustion reaction of the blend showed an increasing trend. The Coats–Redfern model used in this study fit well with the experimental results. As the BD addition increased from 5wt% to 10wt%, the activation energy of combustion reactions decreased from 68.50 to 66.74 kJ/mol for SH, 118.34 to 110.75 kJ/mol for PL, and 146.80 to 122.80 kJ/mol for YQ. These results also provide theoretical support for the practical application of blast furnace dust for blast furnace injection.

**Keywords:** thermogravimetric; bag dust; characteristic parameters; combustion properties; kinetic model

### 1. Introduction

Since the 1990s, China's steel industry has undergone rapid changes. The iron and steel industry now plays a key role in China's national economy [1]. With the development of steel enterprises, energy-saving enhancements, and emissions reductions, the introduction of renewable energy into the ironmaking process has become an important research direction. Such research efforts include increasing the productivity of blast furnaces, reducing costs, implementing green manufacturing techniques, and comprehensively utilizing solid wastes [2–3]. In the modern blast furnace ironmaking process, pulverized coal is usually injected to replace part of the coke. Pulverized coal injection can reduce the coke ratio and improve the blast furnace smelting conditions. Therefore, blast furnace coal injection has been widely adopted by iron and steel enterprises [4].

Blast furnace dust represents some of the solid emissions generated during the blast furnace smelting process. Iron and carbon account for approximately one-half of the total dust; the rest is in the form of oxides such as calcium oxide, silicon oxide, aluminum oxide, and magnesium oxide. The main advantages of blast furnace dust are its light mass and small particle size [5–6]. The bag dust used in the present work is one type of blast furnace ash. The rational utilization of blast furnace dust has always been one of the problems confronting iron and steel plants. In the past, blast furnace dust was mainly reused as an iron-containing raw material for sintering or pelletizing. Although these methods are relatively simple and do not require additional equipment, they also bring certain disadvantages, resulting in problems such as non-uniform sintering mixtures, reduced sinter quality, and diminished production [7–8]. Because of the fine dust characteristics of the bag dust, iron dust and coal dust can be

Corresponding authors: Xiao-jun Ning E-mail: ningxj@ustb.edu.cn; Guang-wei Wang E-mail: wgw676@163.com  
© University of Science and Technology Beijing and Springer-Verlag GmbH Germany, part of Springer Nature 2018

mixed together with coal powder and injected into a blast furnace without adding any extra equipment. After the bag dust is mixed with the pulverized coal, the mixture is sprayed into the blast furnace, which can more effectively recycle the iron and carbon present in the dust and is the best method for effectively utilizing the bag dust [9].

As a by-product of ironmaking, blast furnace dust contains very complex components, so many experts and scholars have carried out detailed research on the characteristics of bag dust. Zhong *et al.* [10] studied the carbon structure and combustion properties of blast furnace dust using X-ray diffraction and thermogravimetric analysis. Shen *et al.* [11] found that blast furnace dust can be used to prepare nanometer-sized black iron oxide raw materials. Wang *et al.* [12–13] studied the effect of the addition of other substances on pulverized coal combustion and gasification. Zou and Zhao [9] found that, because blast furnace bag dust contains more metal oxides, it will reduce the ignition temperature of coal and improve the combustibility of coal. Yakovlev *et al.* [14] studied the effect of blast furnace flue dust on the physico-mechanical properties of graphite materials. Robinson [15] found that blast furnace dust can be used as a reducing agent to prepare cold-bonded pellets. Zhao *et al.* [16] studied the structural characteristics and combustion performance of carbon structures prepared from blast furnace bag ash. Due to the complexity of dust ash components and the diversity of coal types, it is necessary to conduct more in-depth research on the co-firing of the dust and pulverized coal.

In the present study, we used thermal analysis technology to study the combustion performance of samples of blast furnace bag dust and three kinds of pulverized coals combined in different ratios, under non-isothermal combustion conditions. In addition, the Coats–Redfern model [17] proposed by previous researchers is used to fit the combustion kinetics of pulverized coal and to analyze the activation

energy ( $E_a$ ).

## 2. Experimental

### 2.1. Materials preparation and analysis

The blast furnace flue dust samples used in this study were provided by a steel plant in China. The samples were collected from a bag dust (BD) separator installed in a blast furnace gas cleaning system. Three kinds of more common pulverized coals—Shenhua (SH) bituminous coal, Pingluo (PL) anthracite, and Yangquan (YQ) anthracite—were obtained from various companies. Prior to the experiments, the three coals and the flue dust were first dried at room temperature and then ground to 2 mm or smaller and heated in a drying oven at 378 K for 2 h. The dried samples were further ground and sieved with a vibrating sieve. The samples with a particle size of less than 0.074 mm were selected for bagging and sealing.

The proximate and ultimate analyses of the four samples were conducted in accordance with Chinese standard GB/T 212-2001. The results are shown in Table 1. In accordance with Chinese standard GB/T 212-2008, the ash and volatiles of different samples were prepared in a muffle furnace by air oxidation at 1073 K. The mineral contents of the flue dust were measured with an X-ray fluorescence spectrophotometer (XRF-1800) equipped with an Rh-target X-ray tube and a 4-kW generator; the results are presented in Table 2. Scanning electron microscopy (SEM) performed on an SU8010 was used to observe the morphological structure of the prepared samples. The particle size distribution of the raw materials was determined with an LMS-30 laser particle size analyzer. Raman spectroscopy was used to analyze the intrinsic carbonaceous structure of chars in the pulverized coal. The selectable wavelength was 532 nm, the laser power was 2 mW, and the wavenumber range was 800–3000  $\text{cm}^{-1}$ . The spectrum acquisition time was 60 s.

**Table 1. Proximate and ultimate analyses of coal and bag dust**

wt%

Sample	Proximate analysis				Ultimate analysis				
	FC <sub>ad</sub> <sup>a</sup>	A <sub>ad</sub>	V <sub>ad</sub>	M <sub>ad</sub>	C <sub>ad</sub>	H <sub>ad</sub> <sup>a</sup>	O <sub>ad</sub>	N <sub>ad</sub>	S <sub>ad</sub>
SH	53.694	9.658	28.939	7.709	67.660	4.118	9.720	0.800	0.335
YQ	79.242	11.844	6.928	1.986	80.170	2.805	1.030	1.070	1.095
PL	73.464	15.589	8.522	2.425	77.000	2.802	1.198	0.660	0.320
BD	25.495	66.572	7.567	0.366	31.180	0.459	0.164	0.350	0.909

Note: <sup>a</sup> Calculated by difference. FC—Fixed carbon; A—Ash; V—Volatile matter; M—Moisture; ad—Air drying base.

**Table 2. Ash composition of the bag dust**

wt%

Fe <sub>2</sub> O <sub>3</sub>	CaO	SiO <sub>2</sub>	Al <sub>2</sub> O <sub>3</sub>	SO <sub>3</sub>	K <sub>2</sub> O	ZnO	Cl
61.83	3.35	11.59	6.10	6.30	0.60	4.92	4.46

The BD was blended into the three coal samples at ratios of 5wt% and 10wt%. The sample with BD addition of  $n$ wt% is referred to as  $n$ BD(100- $n$ )coal. For example, SH coal

with a BD addition of 5wt% is recorded as 5BD95SH.

## 2.2. Thermogravimetric analysis

The combustion of samples in this work was carried out using a thermogravimetric analyzer (HCT-3, Henven Scientific Instrument Factory, China) under an air atmosphere. The thermogravimetric analyzer system consists of five parts: reaction system, gas control system, temperature control system, cooling system, and computer real-time recording system. The prepared sample was weighed out into a circular crucible with an inner diameter of 5 mm and a height of 2 mm. The crucible was placed on a platinum basket, and the relationship between the sample mass and the temperature was obtained by program control (TG curve). In this experiment, the heating rate was set to 20 K/min. The gas introduced into the differential heat balance was air. The heating was started from room temperature, and the end temperature was 1173 K; the holding time was 5 min.

## 2.3. Kinetic model

In this experiment, the Coats–Redfern model was used to fit the experimentally measured data. The combustion reaction of the sample was performed under the condition of thermal equilibrium. The kinetic equation satisfied by the co-combustion reaction of coal and bag-type dust can be written as

$$\frac{dx}{dt} = k(T) \cdot f(x) \quad (1)$$

where  $x$  is the conversion rate of the combustion reaction, %;  $T$  is the temperature, K; and  $t$  is the time, min.

The rate constant  $k(T)$  can be considered to follow the Arrhenius equation:

$$k(T) = A \exp\left(-\frac{E}{RT}\right) \quad (2)$$

where  $A$  is a pre-exponential factor;  $E$  is the activation energy of the reaction, kJ/mol; and  $R$  is the gas constant, 8.314 J/(mol·K).

Function  $f(x)$  can be expressed as

$$f(x) = (1-x)^n \quad (3)$$

where  $n$  is the order of the reaction.

The conversion ( $x$ ) is defined as

$$x = \frac{m_0 - m_1}{m_0 - m_\infty} \quad (4)$$

where  $m_0$  is the initial mass of the sample;  $m_1$  is the remaining mass of the sample at the time of the reaction; and  $m_\infty$  is the mass of the sample at the end of the reaction.

The combustion reaction is carried out at a constant temperature increase rate:  $\beta$  ( $\beta = dT/dt$ ). Eqs. (2), (3),

and  $dt = dT/\beta$  are brought into Eq. (1) to obtain the following equation:

$$\frac{dx}{(1-x)^n} = \frac{A}{\beta} \exp\left(-\frac{E}{RT}\right) dT \quad (5)$$

In the combustion experiment of pulverized coal, the combustion reaction of pulverized coal is a first-order reaction [18]. Therefore, the integration of the aforementioned formula is as follows:

$$\ln\left[-\frac{\ln(1-x)}{T^2}\right] = -\frac{E}{RT} + \ln\frac{AR}{\beta E} \quad (6)$$

A plot of  $1/T$  on the horizontal axis and  $\ln[-\ln(1-x)/T^2]$  on the vertical axis results in a straight line with a slope of  $-E/R$ , from which the activation energy can be calculated.

## 3. Results and discussion

### 3.1. Physical and chemical characteristics

The particle size distribution of the BD is given in Fig. 1, which shows that the particle size of the bag dust is relatively dispersed and that the distribution range is between 0.55 and 151  $\mu\text{m}$ . The specific surface area of the bag dust measured by the laser particle size analyzer was 1.250  $\text{m}^2/\text{m}^3$ .

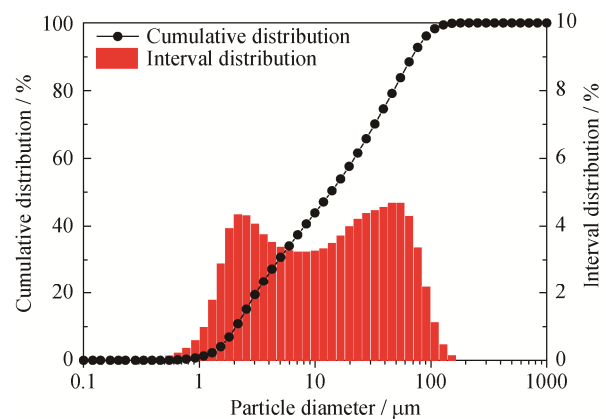


Fig. 1. Particle size distribution of the bag dust.

Raman spectroscopy is often used to characterize the carbon structure of different coals. The Raman spectra of the three types of pulverized coals (Fig. 2) are very similar to that of standard graphite. The Raman spectra of the three types of pulverized coals also have two distinct large peaks, the G band near 1588  $\text{cm}^{-1}$  and the D band near 1350  $\text{cm}^{-1}$ . Because a large overlap exists between the G band and the D band in the Raman spectrum, accurately representing the information in the overlapping region is difficult.

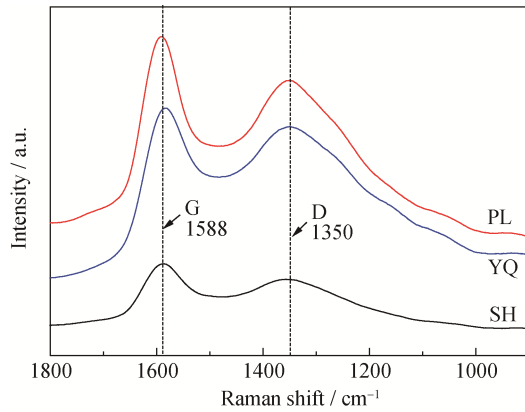


Fig. 2. Raman spectra of the three types of coals.

The Raman analysis method used in the present study was proposed by Li *et al.* [19]. According to this method,

the peaks of several Raman spectra were fit using the Peak-fit software. The results are shown in Fig. 3. The G band of the coal Raman spectrum is mainly due to the aromatic rings breathing. Aromatic compounds containing six or more fused benzene rings but less than in graphite will contribute to the observed D band in the Raman spectrum. The three bands in the region between the G and D bands ( $G_R + V_L + V_R$ ) mainly represent aromatic half-quadrant ring breaths of aromatic ring systems with two or more fused benzene rings. A  $G_L$  band appears at approximately  $1700\text{ cm}^{-1}$ , which mainly represents the carbonyl structure in charcoal. One band at  $1185\text{ cm}^{-1}$  was named the S band to represent  $sp^2$ - $sp^3$  carbonaceous structure in coal. The remaining three bands,  $S_L$ ,  $S_R$ , and R, are attributed to the contribution of ether, benzene-related, and benzene-associated structures, respectively.

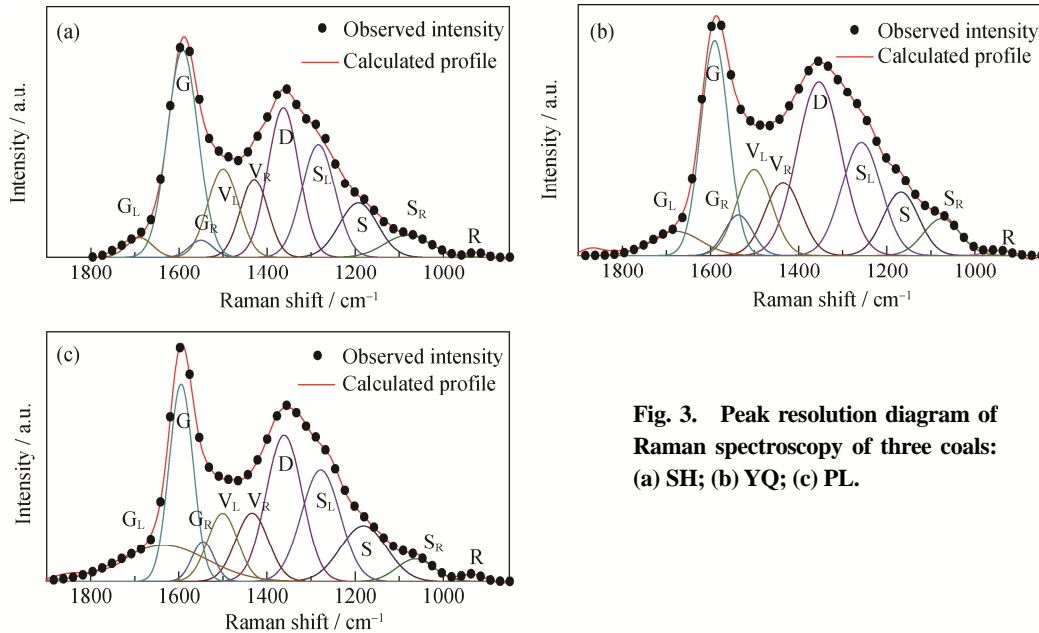


Fig. 3. Peak resolution diagram of Raman spectroscopy of three coals: (a) SH; (b) YQ; (c) PL.

SEM was used to observe the particle shape and surface structure of pulverized coal and bag dust. Fig. 4 shows SEM micrographs of four samples at different observation magnifications. Similarities and differences among the four samples are evident in Fig. 4. Because the three types of pulverized coals were broken and ground, their particle sizes are below 200 mesh. Under low magnification, the pulverized coal exhibits a finer and more uniform particle size. The particle surface of the BD sample is dense, with no apparent pores, and the sample surface is relatively smooth. Although the surface of the SH sample is smooth, numerous cracks are present. The PL and YQ sample surfaces are denser; however, the surface of the PL sample is smoother than that of the YQ sample.

### 3.2. Thermogravimetric analysis of coal and bag dust

The combustion of the four samples was carried out at a heating rate of  $20\text{ K/min}$ . Their conversion curves and conversion rate curves are shown in Fig. 5. Because the samples were dry, they exhibited a high initial conversion temperature; the conversion intervals were between  $300$  and  $900^\circ\text{C}$ . For the four samples, the combustion process can be divided into three stages. In the first stage (the stage where the conversion curve is substantially maintained as the temperature increases), the quality of the sample slightly fluctuates because of the passage of gas. In the second stage (the stage corresponding to the continuous decline of the conversion curve), which represents the sample combustion process, the quality of the pulverized coal rapidly decreases. In the third

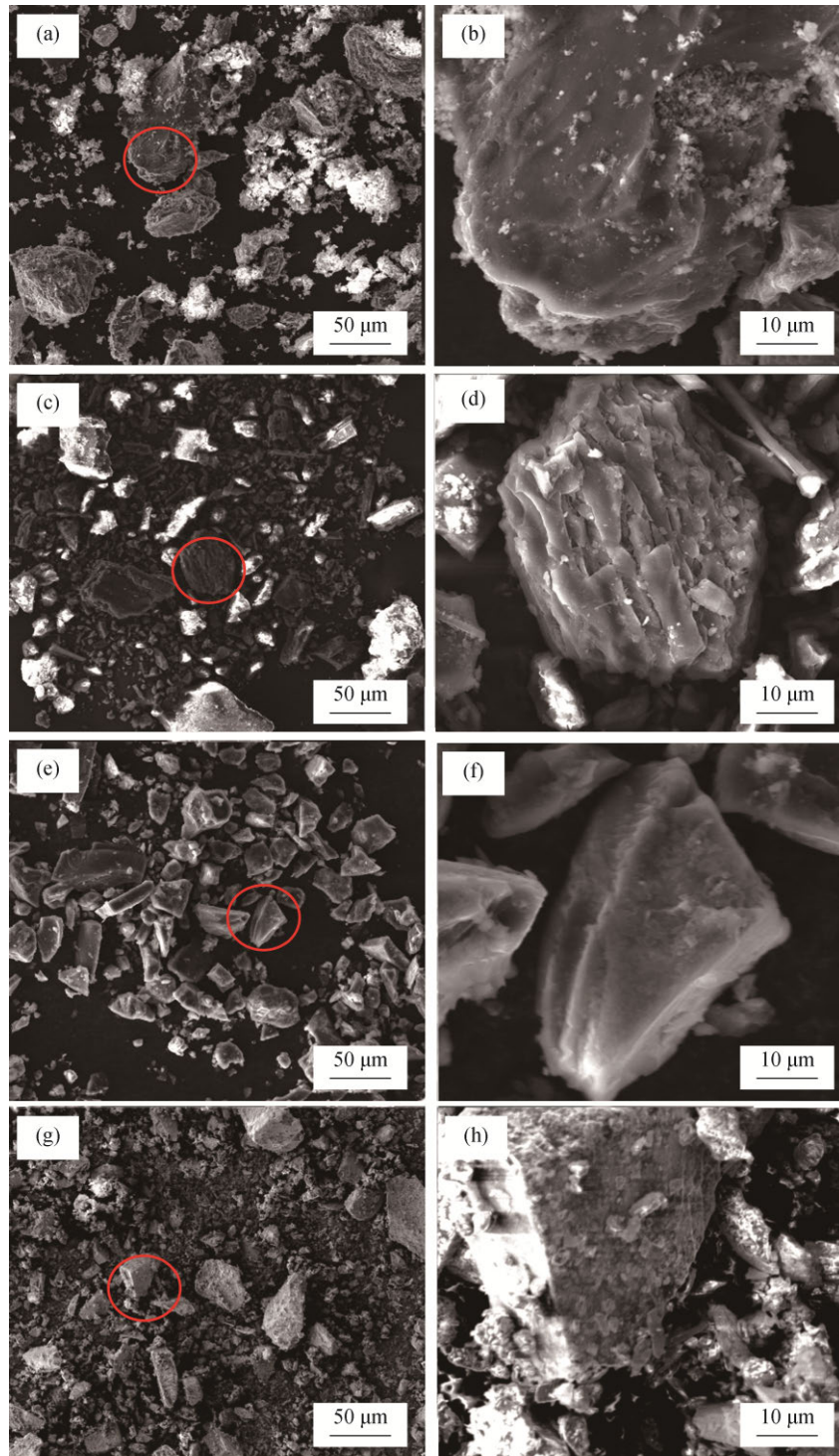


Fig. 4. SEM images of different samples at different magnifications: (a, b) BD; (c, d) SH; (e, f) PL; (g, h) YQ.

stage (the stage in which the conversion curve drops to the lowest and remains at this level), the combustion reaction is completed, the curve is basically flat, and the remaining solid is ash. Fig. 5(a) shows a small peak between 500 and 600°C, likely due to the evaporation of water (hydrocarbons gradually volatilize in the form of volatiles). From Fig. 5 we can see that the conversion curves of the three samples BD,

PL, and YQ did not change significantly before 400°C. The conversion of SH coal begins at 300°C and its inflection point appears at around 600°C. From the curves, all stages of combustion of the three types of pulverized coal are cross-cutting; no clear dividing line is observed, and the conversion rate curves of the combustion stage show a single large peak. Because the peak heights of the four peaks

differ, we concluded that the degree of combustion of these four samples decreases in the order PL > YQ > SH > BD. Moreover, with respect to the inflection points of these three coal conversion rate curves, the inflection point of SH coal

is between 500 and 600°C, whereas the PL and YQ curves show an inflection point between 600 and 700°C. Therefore, the flammability of the SH coal is better than that of the PL and YQ coals.

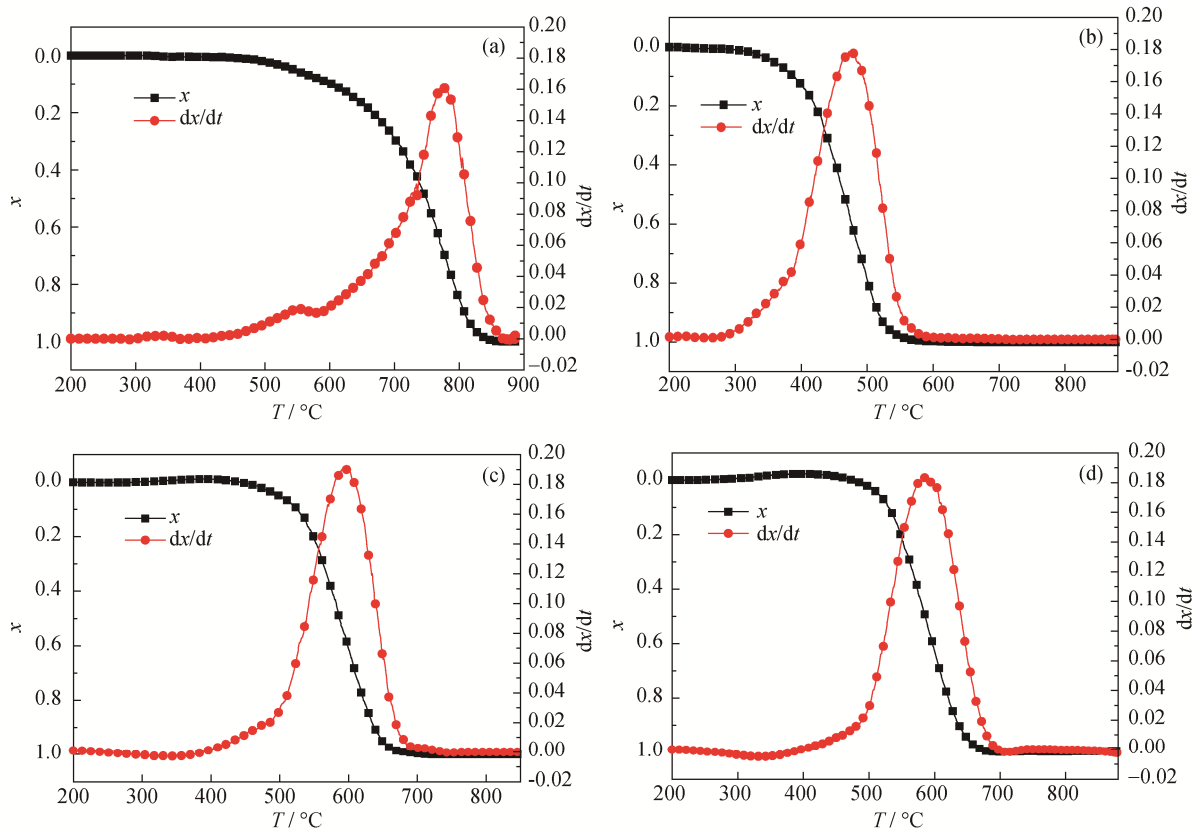


Fig. 5. Combustion curves of the four samples (20 K/min): (a) BD; (b) SH; (c) PL; (d) YQ.

### 3.3. Combustion process of blends

The conversion curves and conversion rate curves of samples SH, PL, YQ, BD, and their blends at a heating rate of 20 K/min are shown in Fig. 6. After the addition of a small amount of bag dust, the combustion curve of the blend was very similar to that of the individual pulverized coal. This result indicates that the combustion processes of the blend and the pulverized coal alone are similar. For the bituminous SH coal, with increasing amount of BD added, the combustion curve of the blend gradually shifted to the right and remained similar to the combustion curve of the bag dust alone, consistent with the traditional combustion law of the mixture. However, for the two anthracite coals, PL (Figs. 6(c) and 6(d)) and YQ (Figs. 6(e) and 6(f)), the slope of the conversion curve of the mixed sample gradually shifts to the left with increasing ratio of the BD. This behavior contradicts the traditional theoretical rules; however, oxides in the bag dust may play a catalytic role in the combustion reaction, and the catalytic

effect may be greater than the effect of the increase in ash [20].

To quantitatively compare the effect of dust ash addition on the combustion characteristics of the three coal samples, we used the ignition temperature of the combustion process ( $T_i$ ), the burnout temperature ( $T_f$ ), the maximum reaction rate ( $R_{\max}$ ), the mean reaction rate ( $R_{\text{mean}}$ ), the ignition index ( $C$ ), the comprehensive combustion characteristic index ( $S$ ), and other parameters [21–22] of the combustion process; these parameters are often used to describe the combustion characteristics of blended coal under different bag gray ratio conditions.

The ignition index  $C$  can represent the reaction parameters of the blend in the early combustion stage. Specifically, a larger  $C$  value indicates better combustibility of the coal sample in the early stage. The  $C$  value can be calculated by the following equation:

$$C = \frac{R_{\max}}{T_i^2} \quad (7)$$

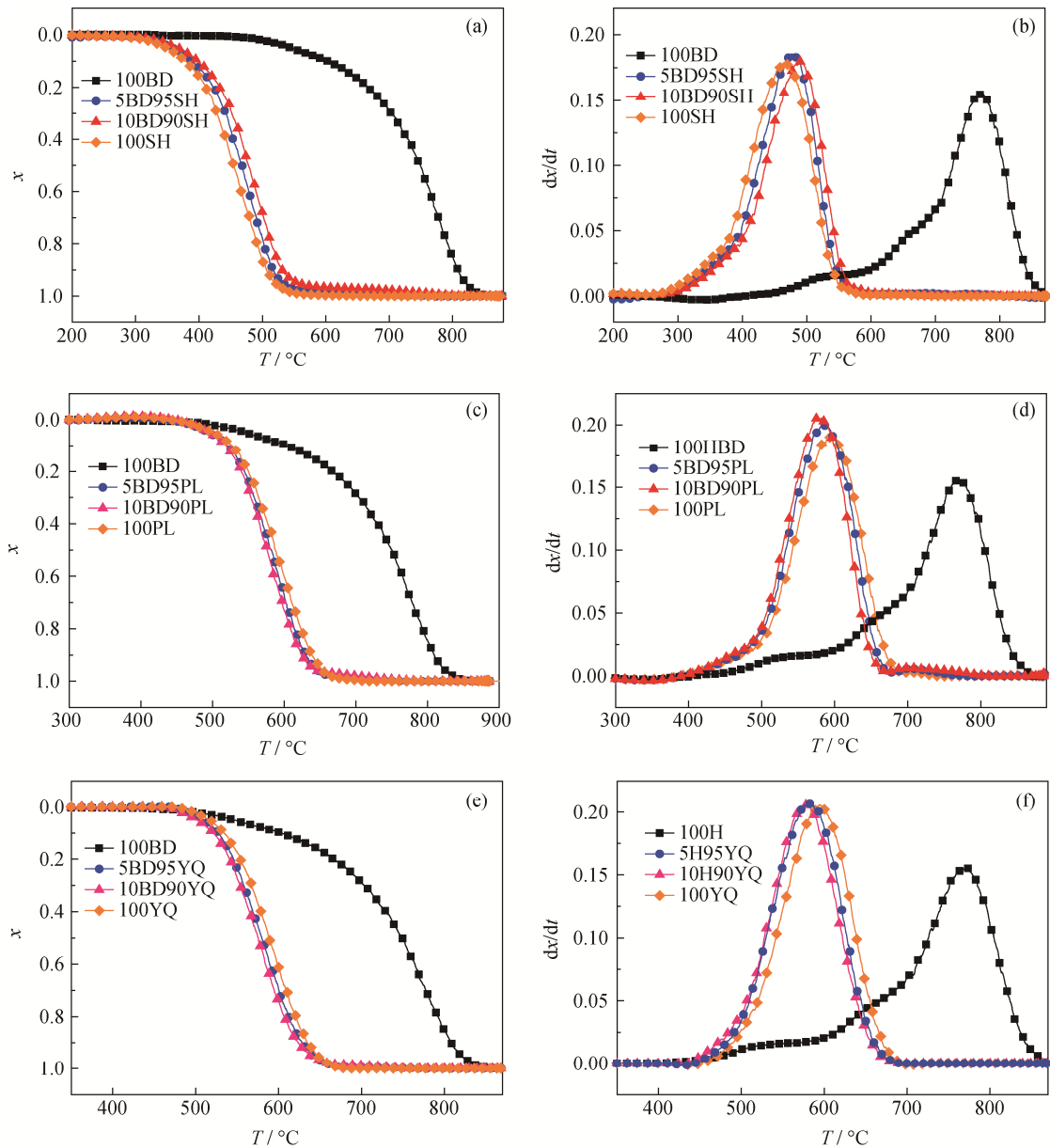


**Fig. 6.** Conversion curves and conversion rate curves for bag dust and coal blends (20 K/min): (a, b) BD + SH; (c, d) BD + PL; (e, f) BD + YQ.

The comprehensive combustion characteristic index  $S$  is an important parameter indicating the comprehensive combustion performance of the blend. The larger the  $S$  value, the better the comprehensive combustion performance of the coal sample. The  $S$  value can be calculated by

$$S = \frac{R_{\max} R_{\text{mean}}}{T_i^2 T_f} \quad (8)$$

The combustion characteristic parameters of the sample, as well as the ignition index and comprehensive combustion characteristic index under a heating rate of 20 K/min, are shown in Table 3. The results in Table 3 show that the magnitude of the  $T_i$  value obeys the order  $\text{BD} > \text{YQ} > \text{PL} > \text{SH}$ ;

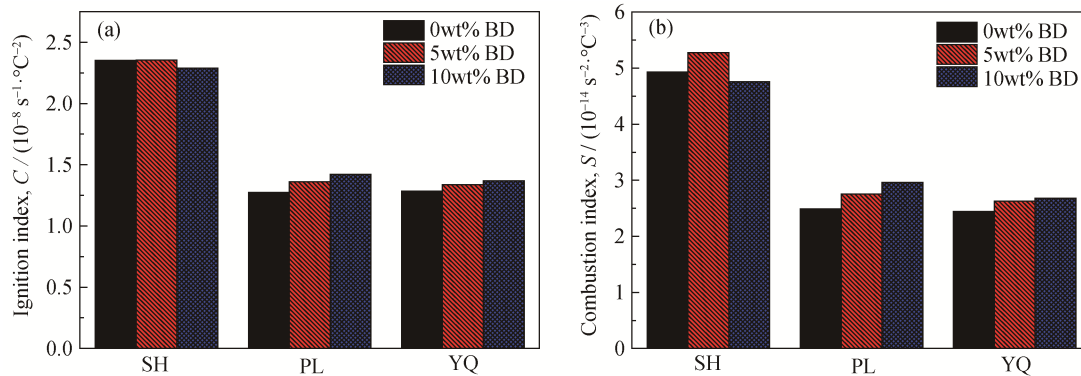
however, a slight difference is observed for  $T_f$ :  $\text{BD} > \text{PL} > \text{YQ} > \text{SH}$ . From the initial temperature and end temperature of the combustion, this change rule is consistent with the qualitative analysis results obtained from the conversion curve. For the SH coal, with the addition of a small amount of dust, the start temperature and the end temperature of the combustion of the blend both shift toward the start and end temperatures of combustion of the bag dust alone, with a slight increase. For the two anthracite coals, with increasing amount of small bag dust addition, the starting temperature and the ending temperature of the sample tend to decrease and the reduction amount differs among the coals.

**Table 3. Combustion characteristic parameters of coal and BD blends (20 K/min)**

Sample	Proportion / wt%	$T_i / ^\circ\text{C}$	$T_f / ^\circ\text{C}$	$R_{\max} / \text{s}^{-1}$	$R_{\text{mean}} / \text{s}^{-1}$	$C / (\text{s}^{-1}\cdot^\circ\text{C}^{-2})$	$S / (\text{s}^{-2}\cdot^\circ\text{C}^{-3})$
BD	100	546.3	820.7	$2.70\times 10^{-3}$	$8.33\times 10^{-4}$	$9.047\times 10^{-9}$	$9.183\times 10^{-15}$
	100	355.0	530.1	$2.96\times 10^{-3}$	$1.12\times 10^{-3}$	$2.353\times 10^{-8}$	$4.927\times 10^{-14}$
SH	95	357.6	533.3	$3.01\times 10^{-3}$	$1.15\times 10^{-3}$	$2.354\times 10^{-8}$	$5.275\times 10^{-14}$
	90	361.5	549.5	$2.99\times 10^{-3}$	$1.13\times 10^{-3}$	$2.288\times 10^{-8}$	$4.755\times 10^{-14}$
PL	100	499.6	650.8	$3.18\times 10^{-3}$	$1.27\times 10^{-3}$	$1.275\times 10^{-8}$	$2.489\times 10^{-14}$
	95	494.6	642.9	$3.33\times 10^{-3}$	$1.30\times 10^{-3}$	$1.361\times 10^{-8}$	$2.753\times 10^{-14}$
	90	494.2	638.9	$3.47\times 10^{-3}$	$1.33\times 10^{-3}$	$1.421\times 10^{-8}$	$2.958\times 10^{-14}$
YQ	100	516.9	646.1	$3.43\times 10^{-3}$	$1.23\times 10^{-3}$	$1.284\times 10^{-8}$	$2.444\times 10^{-14}$
	95	509.5	641.0	$3.47\times 10^{-3}$	$1.26\times 10^{-3}$	$1.337\times 10^{-8}$	$2.628\times 10^{-14}$
	90	502.2	637.7	$3.45\times 10^{-3}$	$1.25\times 10^{-3}$	$1.368\times 10^{-8}$	$2.681\times 10^{-14}$

With the addition of bag dust, there is a difference in the ignition index and comprehensive combustion characteristic index of bituminous coal and anthracite. The results show that, with the addition of bag dust, the combustion performance of the blends improved. The addition amount of the bag dust was plotted against the ignition index  $C$  and the comprehensive combustion characteristic index  $S$  of the blends, as shown in Fig. 7. This plot shows more intuitively that, for anthracite, the ignition index and the

comprehensive combustion index of pulverized coal show a positive correlation with the increase of the amount of BD added. For the SH bituminous coal, with increasing amount of bag dust added, the comprehensive combustion characteristics index of pulverized coal first increase and then decrease. These phenomena indicate that the addition of flue dust can improve the combustion performance of bituminous coal and anthracite by various degrees.

**Fig. 7. Combustion characteristics of the samples: (a) ignition index  $C$ ; (b) combustion characteristic index  $S$ .**

### 3.4. Analysis of kinetic parameters

The Coats–Redfern kinetic model was used to fit the samples during combustion. According to Eq. (6), there is a liner relationship between  $\ln[-\ln(1-x)/T^2]$  and  $1/T$ , in which  $-E/R$  is the slope. The activation energy of the reaction can be calculated from  $-E/R$ . Fig. 8 shows the fitting and calculation results for the samples heated at 20 K/min.

The co-combustion kinetic parameters of the BD and pulverized coal are shown in Table 4. The results show a good linear correlation: the  $R^2$  values are all basically great-

er than 0.99. These results demonstrate that the combustion reaction of the sample is indeed a first-order reaction. The high  $R^2$  values also indicate that the results are very credible. With the increase of bag dust addition (from 5wt% to 10wt%), because the SH bituminous coal itself has a smaller activation energy, its activation energy decreases less: from 68.50 to 66.74 kJ/mol. The activation energy of the two kinds of anthracite (PL and YQ) decreased from 118.34 and 146.80 kJ/mol to 110.75 and 122.80 kJ/mol, respectively. The oxides in the bag dust play a catalytic role in the combustion reaction, and the catalytic effect is greater than the effect of the increase in ash content [23].

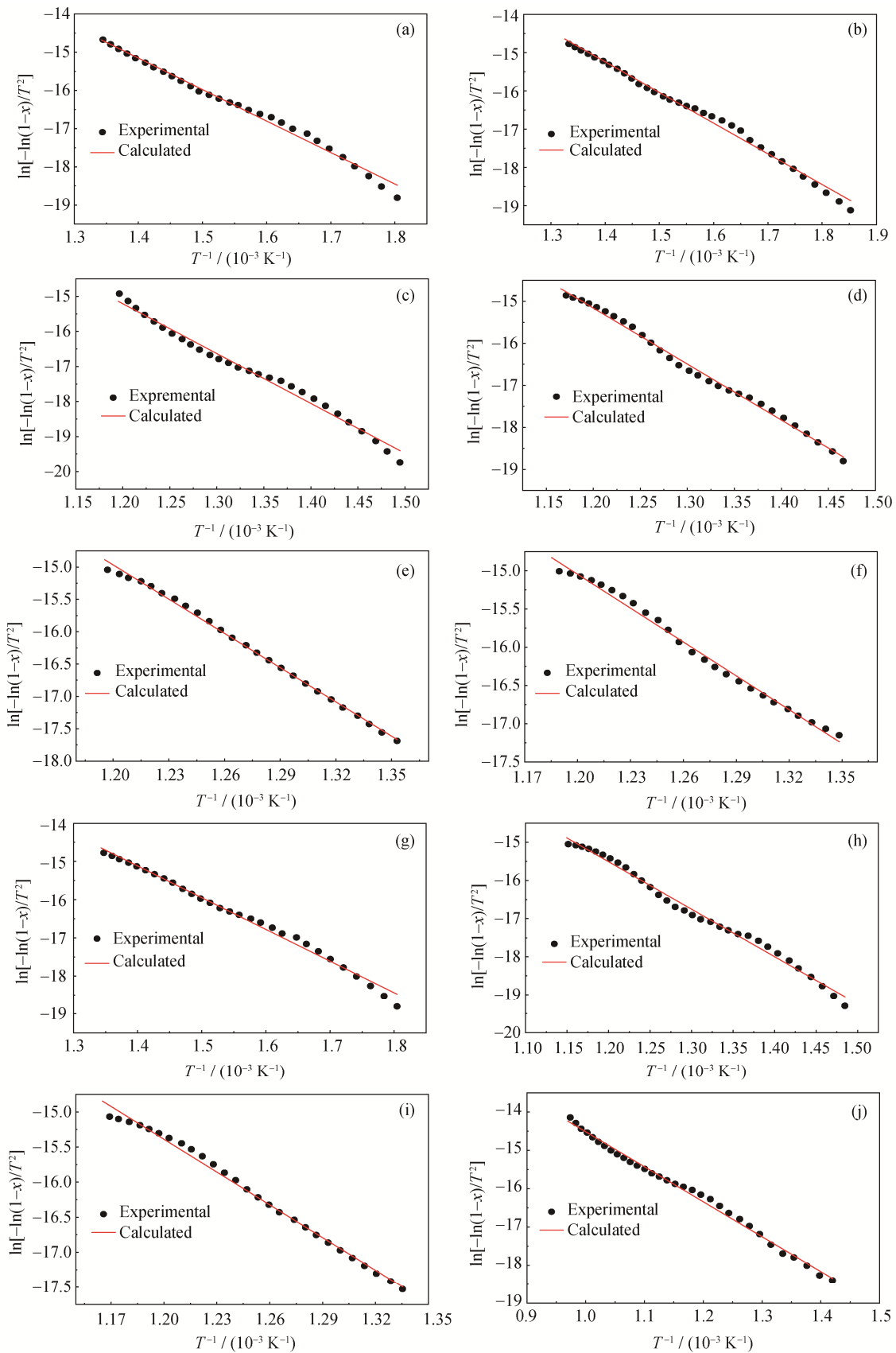


**Fig. 8. Experimental and model profiles for the samples at a heating rate of 20°C/min: (a) 5BD95SH; (b) 10BD90SH; (c) 5BD95PL; (d) 10BD90PL; (e) 5BD95YQ; (f) 10BD90YQ; (g) 100SH; (h) 100PL; (i) 100YQ; (j) 100BD.**

**Table 4. Kinetic parameters of different samples**

Sample	$T/^\circ\text{C}$	$E/(\text{kJ}\cdot\text{mol}^{-1})$	Slope	$R^2$
100SH	286–467	69.01	–8300.6	0.99255
5BD95SH	283–467	68.50	–8238.6	0.99106
10BD90SH	270–473	66.74	–8027.3	0.99295
100PL	407–589	104.10	–12521.1	0.99142
5BD95PL	403–560	118.34	–14233.9	0.98815
10BD90PL	412–597	110.75	–13321.3	0.99498
100YQ	479–582	129.51	–15577.5	0.99325
5BD95YQ	467–560	146.80	–17656.5	0.99737
10BD90YQ	473–571	122.80	–14770.2	0.99220
100BD	431–747	75.93	–9132.4	0.99423

## 4. Conclusions

In this research, the combustion characteristics and kinetic characteristics of the co-combustion of different pulverized coals and BD were studied. The carbonaceous structure strongly influences the combustibility of the samples. Among the four samples, SH exhibits the best combustibility, PL and YQ are slightly weaker, and the BD exhibits poor combustibility. The higher oxide content in pulverized coals plays a catalytic role and promotes the combustion of coal. With the addition of BD, the comprehensive combustion characteristics of pulverized coal improved, which is beneficial to the combustion. The Coats–Redfern model used in this study fits well with the experimental results. As the BD addition increased from 5wt% to 10wt%, the activation energy of combustion reactions decreased from 68.50 to 66.74 kJ/mol for SH, 118.34 to 110.75 kJ/mol for PL, and 146.80 to 122.80 kJ/mol for YQ.

## Acknowledgements

This work was supported by the Natural Science Foundation for Young Scientists of China (No. 51804026), the Young Elite Scientists Sponsorship Program by China Association for Science and Technology (No. 2017QNRC001), and the National Natural Science Foundation of China (No. 51774032).

## References

- [1] Q.Q. Chen, Y. Gu, Z.Y. Tang, W. Wei, and Y.H. Sun, Assessment of low-carbon iron and steel production with CO<sub>2</sub> recycling and utilization technologies: A case study in China, *Appl. Energy*, 220(2018), p. 192.
- [2] G.W. Wang, J.L. Zhang, J.G. Shao, Z.J. Liu, G.H. Zhang, T. Xu, J. Guo, H.Y. Wang, R.S. Xu, and H. Lin, Thermal behavior and kinetic analysis of co-combustion of waste biomass/low rank coal blends, *Energy Convers. Manage.*, 124(2016), p. 414.
- [3] S. Ren, S.L. Li, J. Yang, H.M. Long, J. Yang, M. Kong, and Z.L. Cai, Poisoning effects of KCl and As<sub>2</sub>O<sub>3</sub> on selective catalytic reduction of NO with NH<sub>3</sub> over Mn–Ce/AC catalysts at low temperature, *Chem. Eng. J.*, 351(2018), p. 540.
- [4] U. Leimalm, M. Lundgren, L.S. Okvist, and B. Bjorkman, Off-gas dust in an experimental blast furnace part 1: Characterization of flue dust, sludge and shaft fines, *ISIJ Int.*, 50(2010), No. 11, p. 1560.
- [5] C. Lanzerstorfer, B. Bamberger-Strassmayr, and K. Pilz, Recycling of blast furnace dust in the iron ore sintering process: Investigation of coke breeze substitution and the influence on off-gas emissions, *ISIJ Int.*, 55(2015), No. 4, p. 758.
- [6] V. Trinkel, O. Mallow, P. Aschenbrenner, H. Rechberger, and J. Fellner, Characterization of blast furnace sludge with respect to heavy metal distribution, *Ind. Eng. Chem. Res.*, 55(2016), No. 19, p. 5590.
- [7] N.A. El-Hussiny, M.E.H. Shalabi, Effect of recycling blast furnace flue dust as pellets on the sintering performance, *Sci. Sintering*, 42(2010), No. 3, p. 269.
- [8] P.K. Singh, P.K. Katiyar, A.L. Kumar, B. Chaithnya, and S. Pramanik, Effect of sintering performance of the utilization of blast furnace solid wastes as pellets, *Procedia Mater. Sci.*, 5(2014), p. 2468.
- [9] C. Zou and J.X. Zhao, Investigation of iron-containing powder on coal combustion behavior, *J. Energy Inst.*, 90(2017), No. 5, p. 797.
- [10] Y.W. Zhong, X.L. Qiu, J.T. Gao, and Z.C. Guo, Structural characterization of carbon in blast furnace flue dust and its reactivity in combustion, *Energy Fuels*, 31(2017), No. 8, p. 8415.
- [11] L.Z. Shen, Y.S. Qiao, Y. Guo, and J.R. Tan, Preparation of nanometer-sized black iron oxide pigment by recycling of blast furnace flue dust, *J. Hazard. Mater.*, 177(2010), No. 1-3, p. 495.
- [12] G.W. Wang, J.L. Zhang, G.H. Zhang, X.J. Ning, X.Y. Li, Z.J. Liu, and J. Guo, Experimental and kinetic studies on co-gasification of petroleum coke and biomass char blends, *Energy*, 131(2017), p. 27.
- [13] G.W. Wang, J.L. Zhang, J.G. Shao, and S. Ren, Characterisation and model fitting kinetic analysis of coal/biomass co-combustion, *Thermochim. Acta*, 591(2014), p. 68.
- [14] G. Yakovlev, V. Khozin, I. Polyanskikh, J. Keriene, A. Gordina, and T. Petrova, Utilization of blast furnace flue dust while modifying gypsum binders with carbon nanostructures, [in] The 9th Conference “Environmental Engineering”, Vilnius, 2014, art. No. enviro.2014.025.
- [15] R. Robinson, High temperature properties of by-product cold

- bonded pellets containing blast furnace flue dust, *Thermochim. Acta*, 432(2005), No. 1, p. 112.
- [16] D. Zhao, J.L. Zhang, G.W. Wang, A.N. Conejo, R.S. Xu, H.Y. Wang, and J.B. Zhong, Structure characteristics and combustibility of carbonaceous materials from blast furnace flue dust, *Appl. Therm. Eng.*, 108(2016), p. 1168.
- [17] A.W. Coats and J. Redfern, Kinetic parameters from thermogravimetric data, *Nature*, 201(1964), p. 68.
- [18] G.Q. Liu, Q.C. Liu, X.Q. Wang, F. Meng, S. Ren, and Z.P. Ji, Combustion characteristics and kinetics of anthracite blending with pine sawdust, *J. Iron Steel Res. Int.*, 22(2015), No. 9, p. 812.
- [19] X.J. Li, J. Hayashi, and C.Z. Li, FT-Raman spectroscopic study of the evolution of char structure during the pyrolysis of a Victorian brown coal, *Fuel*, 85(2006), No. 12-13, p. 1700.
- [20] T.S. Farrow, C.G. Sun, and C.E. Snape. Impact of biomass char on coal char burn-out under air and oxy-fuel conditions, *Fuel*, 114(2013), p. 128.
- [21] X.G. Li, B.G. Ma, L. Xu, Z.W. Hu, and X.G. Wang, Thermogravimetric analysis of the co-combustion of the blends with high ash coal and waste tyres, *Thermochim. Acta*, 441(2006), No. 1, p. 79.
- [22] B.G. Ma, X.G. Li, L. Xu, K. Wang, and X.G. Wang, Investigation on catalyzed combustion of high ash coal by thermogravimetric analysis, *Thermochim. Acta*, 445(2006), No. 1, p. 19.
- [23] Z.T. Yao, X.S. Ji, P.K. Sarker, J.H. Tang, L.Q. Ge, M.S. Xia, and Y.Q. Xi, A comprehensive review on the applications of coal fly ash, *Earth Sci. Rev.*, 141(2015), p. 105.